Synthesis of Cellulose Nano Fiber from Palmyrah Fruit Fiber and its Applicability as a Reinforcement Agent on Starch Based Biodegradable Film

Article *in* Ceylon Journal of Science · June 2024

DOI: 10.4038/cjs.v53i3.8257

CITATIONS
2

READS
88

4 authors:

Akshana Roshan
Sabaragamuwa University of Sri Lanka
3 PUBLICATIONS **2** CITATIONS
SEE PROFILE

Sobini Nithiyananthan
Palmyrah Research Institute
18 PUBLICATIONS **12** CITATIONS
SEE PROFILE

Kirushanthi Thangavel
Palmyrah Research Institute
25 PUBLICATIONS **16** CITATIONS
SEE PROFILE

Srithayalan Srivijeindran
Palmyrah Research Institute
70 PUBLICATIONS **175** CITATIONS
SEE PROFILE

RESEARCH ARTICLE

Synthesis of Cellulose Nano Fiber from Palmyrah Fruit Fiber and its Applicability as a Reinforcement Agent on Starch Based Biodegradable Film

R.S. Akshana, N. Sobini*, T. Kirushanthi and S. Srivijeindran

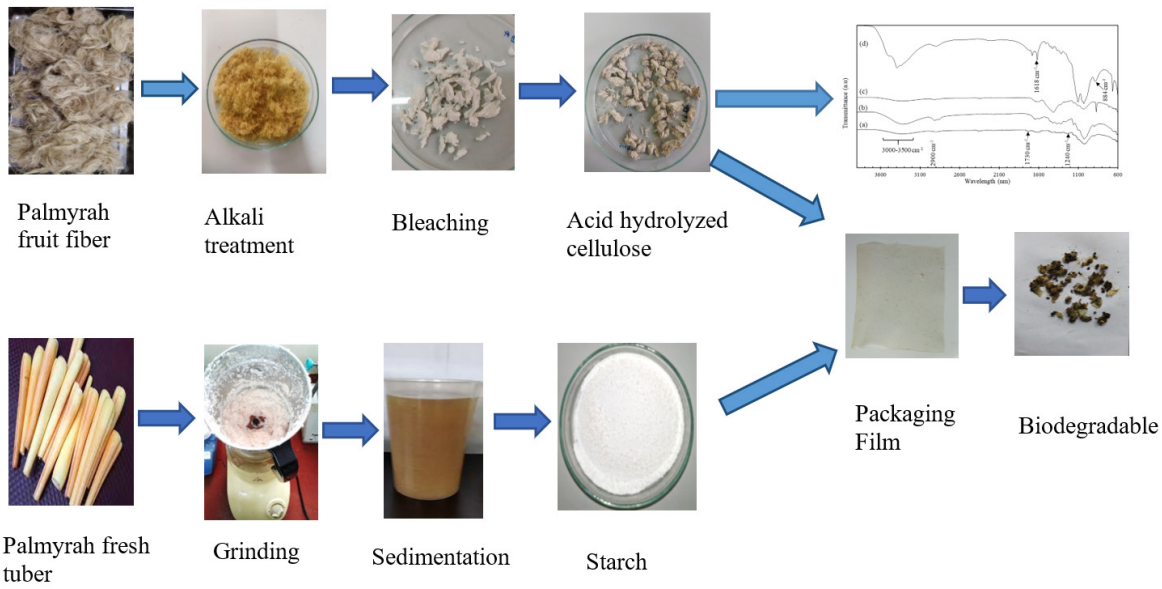

Highlights

- The yield of cellulose from Palmyrah fruit fiber was 37.890±0.008 %.
- Nearly 5-12 days taken for the complete biodegradation of the films.
- Particles Size Distribution results revealed that nano-sized cellulose fiber was synthesized successfully.
- The tensile strength of the film increased up to the incorporation of 1.5% of cellulose.
- Water vapour transmission rate decreased with the incorporation of cellulose.

Ceylon Journal of Science 53 (3) 2024: 313-320
DOI: https://doi.org/10.4038/cjs.v53i3.8257

RESEARCH ARTICLE

Synthesis of Cellulose Nano Fiber from Palmyrah Fruit Fiber and its Applicability as a Reinforcement Agent on Starch Based Biodegradable Film

R.S. Akshana[1], N. Sobini[2,*], T. Kirushanthi[2] and S. Srivijeindran[2]

[1]Department of Food Science and Technology, Faculty of Applied Sciences, Sabaragamuwa University of Sri Lanka, P.P. Box 02, Belihuloya, Sri Lanka
[2]Palmyrah Research Institute, Kandy Road, Kaithady, Jaffna, Sri Lanka

Received: 13.10.2023; Accepted: 10.05.2024

Abstract: The global trend in packaging is shifting towards environmentally friendly, natural materials that decompose easily. Among the bio-based packaging materials, starch is a renewable, biodegradable, bio-compatible, and easily accessible source. However, starch-based biodegradable films depict weak mechanical properties compared with synthetic polymers. This problem can be solved by incorporating reinforcement fillers into the starch matrix. Palmyrah fruit (*Borassus flabellifer* L.) waste can be a good source to obtain fillers due to its high cellulose content. The aim of the study was to investigate the reinforcement of starch-based biodegradable films with the incorporation of pure cellulose nanofiber (CNF) obtained from palmyrah fruit fiber (PFF). Chemical treatments such as alkaline treatment (4% NaOH), bleaching [1% $Ca(OCl)_2$], and acid hydrolysis (10 $moldm^{-3}$ H_2SO_4) were done successively to obtain pure CNF from PFF. CNF was characterized using FTIR and particle size distribution (PSD) was analyzed by granulometry. The yield of CNF from PFF was 37.890±0.008 %. The results of FTIR depicted CNF was synthesized successfully. Five different biodegradable films were prepared by varying the amount of palmyrah tuber starch (4.5-2.5 w/w %) and CNF (0.0-2.0 w/w %) while the amount of glycerin (1.5 w/w %) and gelatin (1 w/w %) were kept constant. PSD results revealed that nano-sized CNF (10-100 nm) was synthesized successfully. The optimized film was selected based on the tensile strength and low water vapor transmission rate. Optimized film formulation, with palmyra tuber starch (3 w/w %) and CNF (1.5 w/w %) showed desirable physical, mechanical and optical properties, including the thickness, moisture content, water vapor transmission rate, water uptake, transparency at 600 nm, water activity, water solubility and tensile strength of 0.192±0.004 mm, 11.07±0.04 %, 3.870±0.005 g/m^2.day, 22.34±0.05 %, 3.97±0.01 %, 0.440±0.001, 51.68±0.140 % and 9.55 MPa respectively. All films showed excellent soil biodegradability within two weeks. In conclusion, palmyra fruit CNF can be effectively used to reinforce starch-based biodegradable packaging films.

***Keywords*:** Cellulose nanofibers; Palmyrah tuber starch; Tensile strength; Water vapor transmission rate; Biodegradable film

INTRODUCTION

In the food supply chain, food packaging plays a significant role because it ensures that consumers receive high-quality, safe food products (Loo & Sarbon, 2020). Active packaging, biodegradable packaging, intelligent packaging, and edible packaging are a few examples of novel storage strategies that have enormous research potential. Since environmentally friendly natural materials are easily degradable, the global trend is now giving its attention to packaging materials that could be easily decomposed. Starch is a source that is readily available, renewable, biodegradable, and nontoxic among bio-based packaging materials. However, biodegradable films made of starch have poor mechanical characteristics (Cheng et al., 2021). This issue can be resolved by incorporating reinforcement fillers into the starch matrix. After extracting the pulp from palmyrah fruits, the fiber remains is considered a waste and it consists of 53.4% (w/w) cellulose (Reddy et al., 2016). Cellulose has attracted a lot of interest because of its distinctive qualities, which include high mechanical strength, excellent chemical stability, and simplicity of synthesis, non-hypoallergenic behavior, reinforcement capacity, biodegradability, bio-compatibility and cheap material (Reddy et al., 2016). Thus, it can be effectively used as a reinforcement filler. The aim of the study was to examine the reinforcement of cellulose nanofibers (CNF) made from palmyrah fruit fiber (PFF) into a starch-based biodegradable film.

MATERIALS AND METHODS

Fresh Palmyrah tubers and Palmyrah fruits were collected from Jaffna, Sri Lanka. NaOH (VWR chemicals, Leuven, Belgium), Bleaching powder (Local market, Jaffna, Sri Lanka), Con H_2SO_4 (Sigma-Aldrich, St-Louis, USA) were used to extract CNF from PFF. Gelatine (Motha, Colombo, Sri Lanka) and Glycerine (Little Food, Sri Lanka) were used for the development of biodegradable film.

Extraction of cellulose nanofibers (CNF)

The pulp was removed from palmyrah fruit, and the fibers were separated. The fibers were washed with tap water and sun-dried. They were oven-dried using a hot air oven at 50 ±5 °C. Alkali treatment, bleaching, and acid treatment were done successively to separate the CNF using the method described by Hachaichi et al. (2021) with some modifications. About 5 g of residue was dispersed in 4% NaOH and the suspension was stirred at 80 ± 5 °C for 2 h. After filtering and washing the treatment was repeated.

**Corresponding Author's Email: sobinithi30@gmail.com*
https://orcid.org/0000-0002-3669-3852

The fibers were dried at 50 ±5 °C for 24 hours. Dried fibers were treated at 60-70 °C in 1% $Ca(OCl)_2$ solution. The mixture was stirred at frequent intervals for 1 h and then cooled in the ice bath. The fibers were filtered using cold water. The procedure was repeated four times. The bleached fiber was treated in 10 $moldm^{-3}$ of H_2SO_4 at 40 °C at 600 rpm. Hydrolyzed cellulose was washed 6-8 times by centrifuging at 5000 rpm.

Characterization of cellulose nanofibers (CNF)

FTIR analysis

Raw fiber, bleached fiber, and cellulose fiber samples were finely ground or processed to ensure uniformity and suitability for ATR-FTIR analysis. The Thermo Scientific Nicolet iS10 spectrometer was employed for the analysis. To initiate the analysis, a small amount of each prepared fiber sample was placed onto the ATR crystal. The analysis was conducted in the spectral range of 525 - 4000 cm^{-1}, with a resolution set at 4 cm^{-1}. For each fiber sample, multiple scans were acquired to enhance the signal-to-noise ratio and ensure data reliability. The resulting ATR-FTIR spectra were then processed and analyzed to identify characteristic peaks and functional groups, providing valuable insights into the chemical composition and structural properties of the raw fiber, bleached fiber, and cellulose fiber samples.

XRD analysis

The CNF sample was finely ground and homogenized well. Subsequently, the X-ray diffractometer (Regaku Ultima IV) was configured with specific parameters: a 40 kV X-ray source and 30 mA current were employed to generate the essential X-ray beam. To optimize the X-ray beam for precise diffraction analysis, a K-beta filter was selected. The scan mode was set to continuous, and a scan speed of 2.0000 degrees per minute was chosen, with a goniometer step width of 0.0200 degrees, ensuring data collection with high precision. The scan axis was configured as 2Theta/ Theta, covering a range spanning from 5.0000 to 80.0000 degrees. The control of incident and receiving slits, with openings of 2/3 degrees and 0.3 mm, respectively, allowed for the accurate capture of diffracted X-ray signals. XRD pattern was analyzed. The crystallinity index (*CrI*) of CNF was estimated according to Segal's method (Terinte et al., 2011) (Eq. 1)

$$CrI = 100 \times \frac{I_{002} - I_{am}}{I_{002}} \quad \text{(Eq.1)}$$

Where, I_{002} gives the maximum intensity of the peak corresponding to the plane in the sample with the Miller indices 200 at a 2Θ angle of between 22-24 degrees and I_{am} represents the intensity of diffraction of the non-crystalline material, which is taken at an angle of about 18 degrees 2Θ in the valley between the peaks.

Formulations of different biodegradable films

Biodegradable films were prepared using the ingredients as shown in the table 1. Ingredients were mixed at 80 °C for 20 minutes until gelatinization. The solution was cooled and poured on a 25 x 15 cm^2 tray and kept at 40 °C in a hot air oven for 48 h.

Table 1: Formulation of different biodegradable films

Film	Starch (g)	*CNF (g)	Gelatin (g)	Glycerin (g)	Water (mL)
F1	4.5	0.0	1	1.5	93
F2	4.0	0.5	1	1.5	93
F3	3.5	1.0	1	1.5	93
F4	3.0	1.5	1	1.5	93
F5	2.5	2.0	1	1.5	93

*CNF: Cellulose Nanofiber

Mechanical and physical characterization of films

Water vapor transmission rate (WVTR)

A modified wet cup method was used to determine the WVTR. Distilled water was filled into the cup and was sealed by the film. The cup was placed in the desiccator. Silica gel was put into the desiccator to control the Relative humidity (RH). This experiment was conducted at 53.6% relative humidity and 23.5 °C. The cups were periodically removed and then weighed. The WVTR was calculated by the following equation described in Basha et al. (2011).

$$WVTR = \frac{w*t}{A} \quad \text{(Eq.2)}$$

where, WVTR: water vapor transmission rate (g/m^2. d), w: weight change (g), t: time (d), and A: test area (m^2).

Water solubility (WS)

A modified weight loss method was used to determine the water solubility. About 2 cm × 2 cm specimens were weighed and dissolved in distilled water for 24 h. After 24 h, specimens were removed and dried at 90 °C till a constant weight was attained. WS was determined by the following equation described by Niu et al. (2021).

$$WS = \frac{(M1 - M2)}{M1} \quad \text{(Eq.3)}$$

where, M1: Initial weight (dry basis) and M2: Final weight (dry basis).

Water activity (a_w)

Films were cut into small pieces. Water activity was measured using a water activity meter (LabTouch-aw, novasina, India).

Moisture content (MC)

About 2.0 cm x 2.0 cm specimens were used to determine the moisture content. The specimens were placed in an oven at 110 °C until a constant dry weight was attained. MC was determined using the following equation stated by Marichelvam et al. (2019) as follows,

$$MC(\%) = \frac{(Wi - Wf)*100}{Wi} \quad \text{(Eq.4)}$$

Where, Wi: Initial weight and Wf: Final weight.

Thickness

The thickness of the film was measured at five different points of the films using a Micrometer (INGCO, HMM0025-ING, China), and the average thickness was calculated.

Transparency

Film transparency was determined using a UV-Vis spectrophotometer. The film samples were fixed in the cuvette such that the light beam passed through the film. The transparency was determined at 600 nm in triplicate (Han & Floros, 1997) and the values were calculated using the following equation,

$$Transparency(\%) = \frac{Absorbance(600nm)}{Thickness}$$

Biodegradability Test

The biodegradability test was conducted with soil as per the method described in Marichelvam *et al*. (2019). The specimens were cut into 2 cm x 2 cm pieces. Soil which is rich in nitrogenous bacteria was taken near the leguminous plant roots and the specimens were buried at 3 cm depth. Buried specimens were taken from the soil to be observed visually for 15 days. Days taken for the complete biodegradation were observed.

Tensile Strength

The tensile strength was measured using a Universal Testing Machine (WEW, Jinan Kason Testing Equipment Co. Ltd, China) using the method described in Tongdeesoontorn et al. (2012).

Statistical analysis

Statistical data were analyzed by using Minitab 19 software. All the analyses were carried out in triplicates and results were obtained as mean ± standard deviation. One-way analysis of variance (ANOVA), Turkey pairwise comparison linear regression analysis was used for statistical analysis with 95% significance confidence interval.

RESULTS AND DISCUSSION

Optimizing the CNF extraction method

Alkaline treatment was done using NaOH to facilitate the solubilizing of lignin from the fibers. Bleaching of fibers was done to remove surface impurities such as lignin and hemicellulose. This was followed by acid hydrolysis to facilitate a larger molecule split into several smaller ones. Sulphuric acid is effective in recovering the maximum yield by hydrolyzing the cellulose (Kong-Win Chang et al., 2018), the yield was 37.89% w/w.

Characterization of CNF

FTIR analysis

FTIR analysis was employed to assess the impacts of alkaline, bleaching, and acid treatments on the fiber's functional groups, bonding types, and chemical components. The FTIR spectroscopic data for both untreated PFF and treated fibers can be observed in Figure 1. All the spectra exhibit a broad band region at 3000 to 3500 cm^{-1}, indicative of the free O–H stretching vibration attributed to the OH group in cellulose molecules (Hajji et al., 2016). Additionally, all spectra feature the characteristic symmetric/ asymmetric C-H stretching vibration around 2900 cm^{-1} which is associated with cellulose components interacting with lignin molecules (Md Salim et al., 2021). The decrease in intensity at this absorption peak, stemming from the removal of lignin content in the fibers, suggests that the alkaline treatment was less effective in eliminating lignin constituents, while the bleaching treatment successfully eliminated lignin.

The FTIR peak detected at 1730 cm^{-1} in the raw PFF sample is linked to the stretching vibration of C=O bonds found in acetyl and uronic ester groups, which can appear from pectin, hemicelluloses, or the ester linkage of carboxylic groups in compounds like ferulic and p-coumaric acids present in lignin and/or hemicellulose (Raju et al., 2023). Simultaneously, the peak at 1240 cm^{-1} observed in the raw PFF spectrum is attributed to the stretching vibration of C–O bonds associated with acetyl or aryl groups within lignin (Cheng et al., 2023). As the fibers undergo chemical treatments, these two peaks gradually diminish in the spectra due to the removal of hemicellulose and lignin during the treatment processes.

The absence of a peak at 1590 cm^{-1}, which corresponds to the C=C stretching of aromatic rings in lignin, after the treatments indicate that the removal of hemicellulose and lignin has taken place (Sayakulu et al., 2022). Additionally, a consistent peak at 1010 cm^{-1} is observed in all spectra, which can be attributed to the skeletal vibration of the C-O-C pyranose ring (Oladipo et al., 2023). The most prominent absorption band at 884 cm^{-1} consistently increases with alkali and bleaching treatments. This band corresponds to the glycosidic –C-H- deformation, including contributions from ring vibrations and –O-H bending (Giri et al., 2021). These characteristics are indicative of the β-glycosidic linkage between anhydroglucose units in cellulose and are more pronounced with the progression of alkali and bleaching treatments (Rosli et al., 2013).

The XRD patterns of CNF samples are shown in Figure 2. The results revealed prominent characteristic diffraction peaks at 16.34°, 22.54°, 28.54°, and 34.9°. Among these peaks, those at 16.34°, 22.58°, and 34.9°, correspond to the crystallographic planes (110), (200) and (004) of cellulosic fiber, as documented by (Yudha et al., 2021) in their XRD analysis of salacca midrib fibers. The pattern consists of crystalline and amorphous peaks, which are types of semi-crystalline material (Huang et al., 2020). The crystallinity index of the CNF from PFF is about 34 %. Notably, the XRD pattern of CNF displays sharp peaks attributed to impurities in the synthesized CNF, which may adversely affect the intensity of the crystalline peaks. Consequently, it is imperative to explore potential methods for identifying the source and eliminating these impurities.

Table 2 and Figure 2 shows the data of particle size distribution of CNF and Particle size distribution of CNF. According to these data, The D10 value for CNF particles is 35.6 nm which means that 10 % of the cellulose particles in the sample are smaller than 35.6 nm in diameter. The D50 value for cellulose particles is 62.3 nm which means that 50 % of the cellulose particles in the sample have a diameter smaller than or equal to 62.3 nm, and the other 50 % have a diameter larger than this value. The D90 value for cellulose particles is 101.5 nm which means that 90 % of

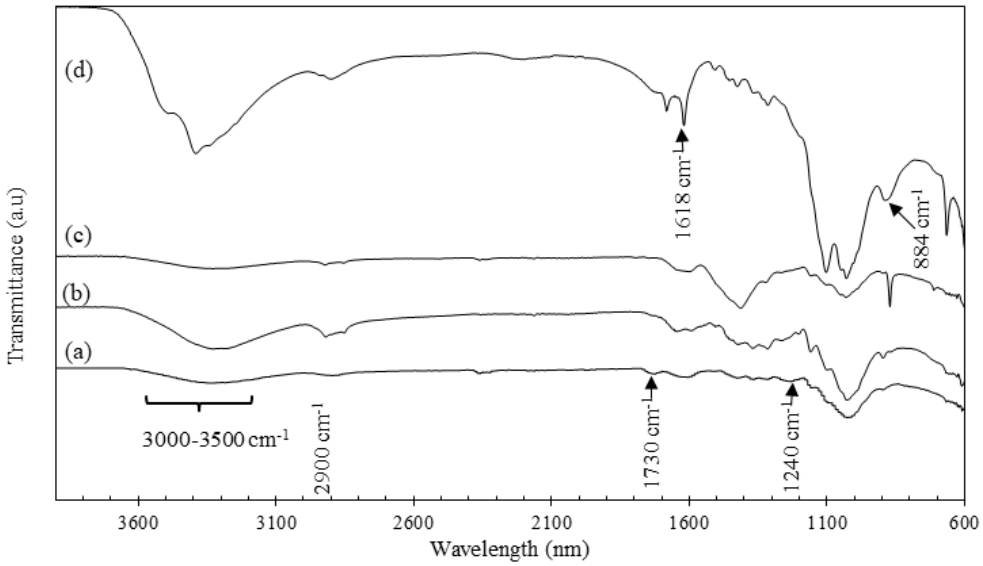

Figure 1: FTIR spectra of (a) raw Palmyrah Fruit fiber (PFF); (b) After alkaline treatment; (c) After bleaching; and (d) Cellulose Nanofiber (CNF) after acid hydrolysis

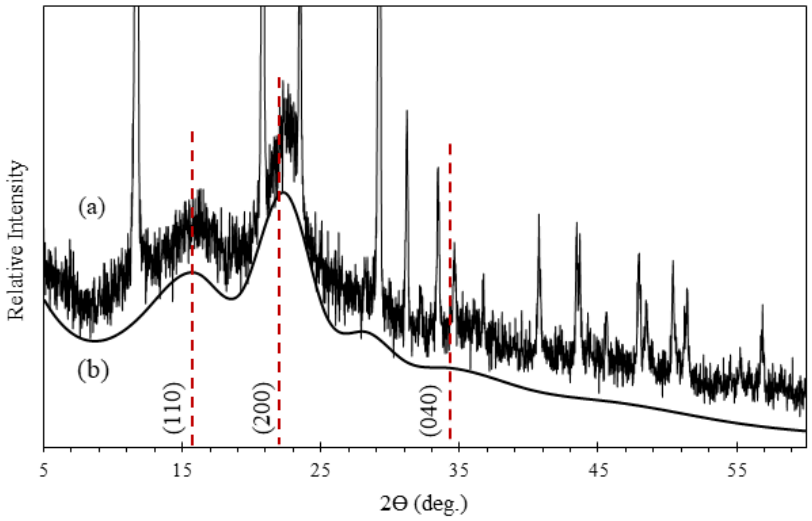

Figure 2: XRD pattern of Celluloose Nanofiber (CNF) sample (a) with background and (b) without background

the cellulose particles in the sample are smaller than 101.5 nm in diameter.

The particles with sizes less than 100 nanometers (nm) are commonly referred to as nanoparticles. The Given data in Table 2 includes D90 values of 101.5 nm for CNF particles, it's accurate to say that these particles are in the nanoscale range but just slightly above the 100 nm threshold. Hence, synthesized CNF particles are in the nanoscale.

Table 2: Data of particle size distribution of Cellulose Nanofiber (CNF).

Sample	D10 (nm)	D50 (nm)	D90 (nm)
Cellulose	35.6	62.3	101.5

Mechanical, physical, and optical properties

The mechanical and physical properties of different formulated films are shown in Figure 4. Figure 4a shows that the addition of CNF progressively raises the TS up to formula 4. Tensile strength of the films with different treatments varied from 4.60 to 9.5 MPa. These results of TS were similar to the study reported by Nordin et al. (2018). The incorporation of 2.0 g of cellulose has resulted in less tensile strength than that of 1.5 g cellulose. The reason could be the excess cellulose that produced agglomerations and an uneven distribution of stress inside the matrix of the film can be responsible for the decrease in TS. According to the study of Savadekar and Mhaske (2012), the addition of more reinforcing agents can also result in phase separation, poor particle distribution, and large agglomerates. However, due to the good dispersion and strong interaction between the cellulose and starch matrix, the TS values obtained were still larger than the values reported for the treatment F1. Thus, values were in accordance with the previous findings as there is a positive relation between incorporation of cellulose into the starch film and its tensile strength up to a certain level CNF concentration was inversely proportional to film transparency (See Figure 4f)

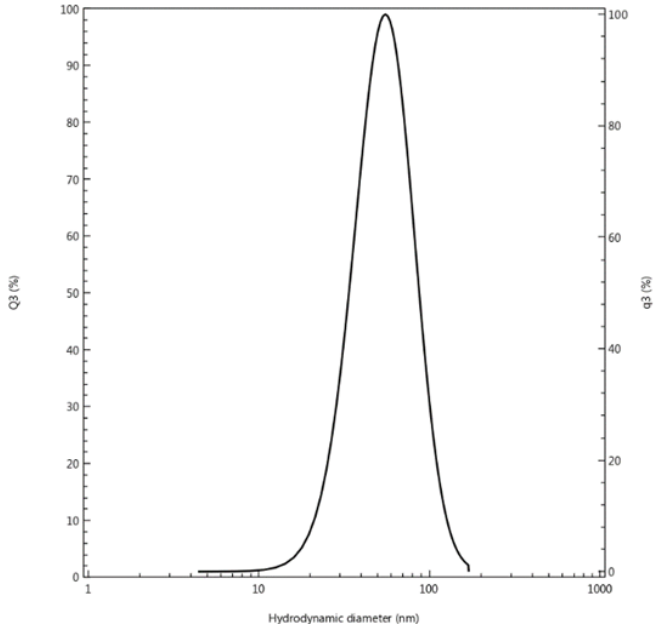

Figure 3: Particle size distribution of Cellulose Nanofiber (CNF).

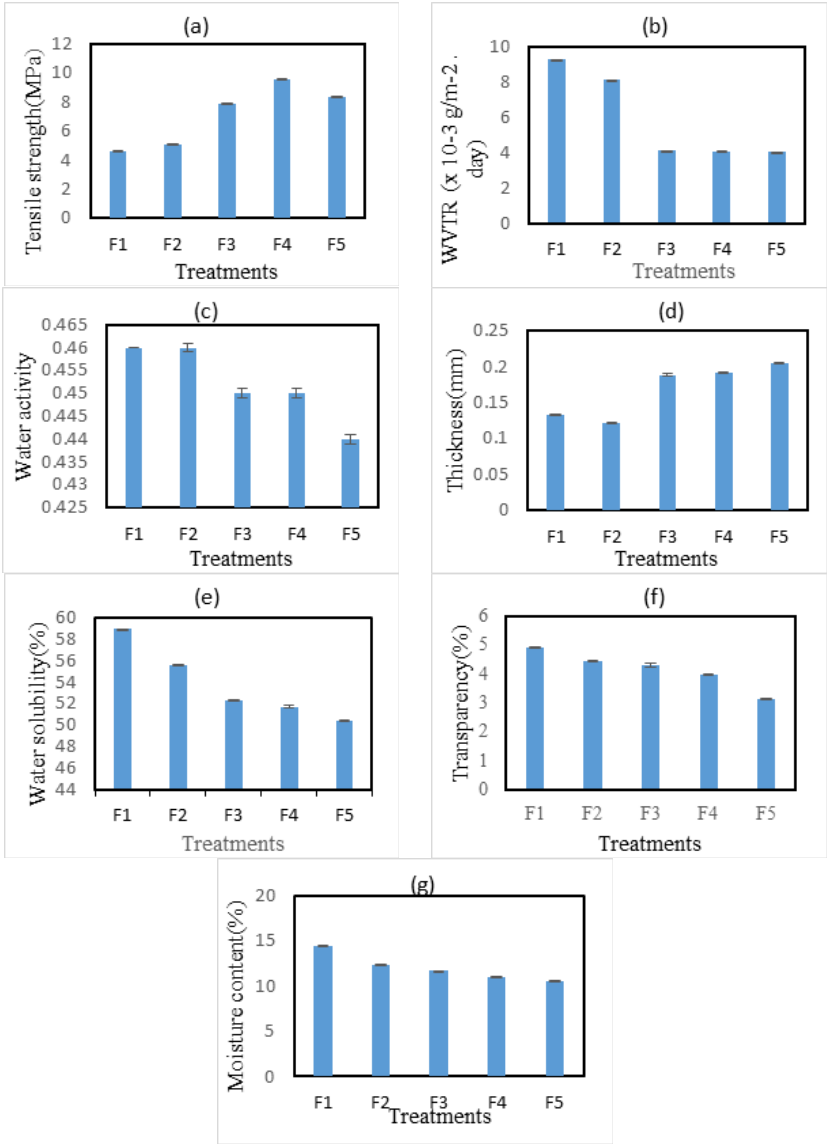

Figure 4: Physical and mechanical parameters (a) tensile strength, (b) water vapour transmission, (c) water activity, (d) thickness, (e) water solubility and (f) transparency (g) moisture content of differently formulated films.

The thickness of the film with the above treatments varied from 0.13 mm to 0.21 mm. Thickness after the treatment F1 reported by Sobini et al. (2022) ranged from 0.11-0.16 mm. (See Figure 4d). The incorporation of CNF into films resulted in a gradual increase in thickness.

The properties such as WVTR, WS, and MC of the treatment F1 were 4.10±0.00 g/m^{-2}.d, 63.09±0.03 %, and 14.43±0.02 % respectively (See Figure 4b, Figure 4e and, Figure 4g respectively). These results were similar to the results reported by Sobini et al. (2022). However, treatment F5 possessed the lowest values of WVTR (3.82±0.003 g/m^{-2}.d), a_{ww} (0.442), and WS (50.37±0.07 %). Moisture content, WVTR, and WS decreased with increasing concentration of CNF. Parameters like MC, WS, and WVTR are dependent on the hydrophilic properties of the film. The more exposed hydroxyl groups attract more water molecules and increase the MC. Hydroxyl groups try to make hydrogen bonds with surrounding water molecules. An extensive block is caused by cellulose after the in-cooperation of cellulose. As a result, the hydrogen bond formation between hydroxyl groups of the film and surrounding water is interrupted which results in the reduction in WVTR, WS, and MC. Thus, the incorporation of CNF into the film has aided in the favorable physical properties of the packaging film.

Biodegradability

The films incorporated with cellulose exhibited an excellent degradation property as shown in figure 5. The biodegradability of cellulose film was low in the first two days. While it was accelerated after two days. The film was changed into small pieces within the first three days and degraded rapidly. It took nearly 5-12 days for the complete biodegradation of the films. Morphological characteristics of the samples buried in the soil is shown in figure 5. Yellow/brown spots appeared on the surface of the starch film after two days of burying in the soil (Čater et al., 2014). After four days of burying, cracks, holes and obvious etches, appeared on the cellulose films, while the film F1 degraded and fragmented quickly. However, the biodegradability of cellulose films took around 5, 10, 10, 11, 12 days for complete soil degradation for F1, F2, F3, F4, F5 respectively. The reason could be that cellulose has a higher crystallinity compared to that of starch. As a result, it takes more time to biodegrade than starch film (Müller et al., 2009).

Optimization of films

Optimized film (F4) was selected based on the highest TS and lower WVTR which showed favorable physical and mechanical properties than that of starch-based films (Sobini et al., 2022).

CONCLUSION

The yield of CNF from PFF was 37.890±0.008 %. Synthesis of CNF was confirmed by FTIR and PSD analysis. PSD results revealed that nano-sized CNF (10-100 nm) was synthesized successfully. XRD analysis of CNF showed its mixture of amorphous and crystalline nature. Film formulation (F4) with palmyrah tuber starch (3 w/w %) and CNF (1.5 w/w %) was optimized as the best formulation based on the highest TS and lower WVTR. It showed desirable physical, mechanical, and optical properties including the thickness, moisture content, water vapor transmission rate, water uptake, and transparency, water activity, water solubility and tensile strength. All films showed excellent soil biodegradability within two weeks. Hence, palmyrah fruit CNF could be effectively utilized to reinforce the starch based biodegradable packaging films.

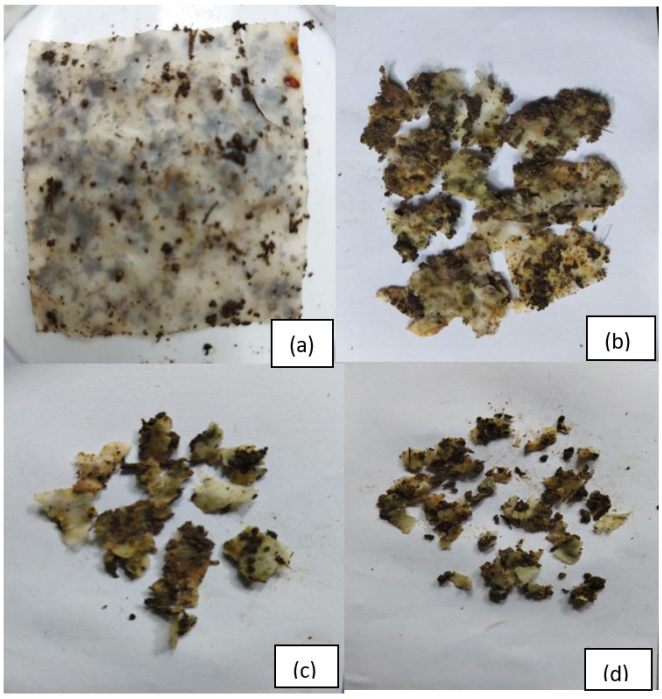

Figure 5: Morphology changes of the film F4 after burying in soil (a) after 2 days, (b) after 4 days, (c) after 6 days, and (d) after 8 days

ACKNOWLEDGEMENT

We thank Palmyrah Research Institute, Jaffna, Sri Lanka, for the financial support.

DECLARATION OF CONFLICT OF INTEREST

The authors declare no conflict of interest.

REFERENCES

Ai, B., Zheng, L., Li, W., Zheng,X., Yang,Y., Xiao,D., Shi,X. & Sheng,Z. (2021) Biodegradable cellulose film prepared from banana pseudo-stem using an Ionic liquid for Mango Preservation, *Frontiers in Plant Science*, **12**: doi:10.3389/fpls.2021.625878.

Astete, J. R., Jimenez-Davalos, J. & Zolla, G. (2021). Determination of hemicellulose, cellulose, holocellulose, and lignin content using FTIR in *Calycophyllum spruceanum* (Benth.) K.Schum. and *Guazuma crinita* Lam. *PLOS ONE*. doi:10.1101/2021.09.01.458618

Basha, R. K., Konno, K., Kani, H. & Kimura, T. (2011). Water vapor transmission rate of biomass-based film materials. *Engineering in Agriculture*, *Environment and Food*, **4**(2): 37-42. doi: 10.1016/S1881-8366(11)80018-2

Blanke, M.M. (2014) Reducing ethylene levels along the food supply chain: A key to reducing food waste? *Journal of the Science of Food and Agriculture*, **94**(12): 2357–2361. doi:10.1002/jsfa.6660.

Čater, M., Zorec, M. & Marinšek Logar, R. (2014) Methods for improving anaerobic lignocellulosic substrates degradation for enhanced biogas production, *Springer Science Reviews*, **2**(1-2):51–61. doi :10.1007/s40362-014-0019-x.

Chandla, N.K., Khatkar, S.K., Singh, S., Saxena, D.C., Jindal, N., Bansal, V. & Wakchaure, N (2020). Tensile strength and solubility studies of edible biodegradable films developed from pseudo-cereal starches: An inclusive comparison with commercial corn starch. *Asian Journal of Dairy and Food Research* [Preprint]. doi:10.18805/ajdfr.dr-1522.

Chang, J.K.W., Duret, X., Berberi, V., Zahedi-Niaki, H., & Lavoie,J .M. (2018) Two-step thermochemical cellulose hydrolysis with partial neutralization for glucose production, *Frontiers in Chemistry*, **6**. doi:10.3389/fchem.2018.00117.

Cheng, H., Chen, L., McClements, D.J., Yang, T., Zhang, Z., Ren, F., Miao, M.,Tian,Y. &

Jin, Z. (2021). Starch-based biodegradable packaging materials: A review of their preparation, characterization, and diverse applications in the food industry. *Trends in Food Science & Technology*, **114**:70-82. doi:10.1016/j.tifs.2021.05.017

Cheng, X.C., Wei,Y.N. Yuan, L.L., Qin,Z., Liu, H.M. & Wang, X.D.(2023)**.** Structural characterization of lignin-carbohydrate complexes from Chinese quince fruits extracted after enzymatic hydrolysis pretreatment. *International Journal of Biological Macromolecules*, **246**: 125664

Fekadu Gemede, H. (2014). Antinutritional factors in plant foods: Potential health benefits and adverse effects, *International Journal of Nutrition and Food Sciences*, **3**(4): 284. doi:10.11648/j.ijnfs.20140304.18.

Giri,J., Adhikari,R. & Sapkota, J. (2021). Structural, thermal and mechanical properties of composites of poly (butylene adipate-co-terephthalate) with wheat straw microcrystalline cellulose. *Polymer Bulleti*n, **78**: 4779-4795.

Hachaichi,A., Kouini,B., Kian,L.K., Asim,M. & Jawaid,M. (2021). Extraction and characterization of microcrystalline cellulose from date palm fibers using successive chemical treatments. *Journal of Polymers and the Environment*, **29**(6), 1990-1999. doi:10.1007/s10924-020-02012-2

Hajji, L., Boukir, A., Assouik,J., Pessanha,S., Figueirinhas, J. L., & Carvalho, M.L. (2016). Artificial aging paper to assess long-term effects of conservative treatment. Monitoring by infrared spectroscopy (ATR-FTIR), X-ray diffraction (XRD), and energy dispersive X-ray fluorescence (EDXRF). *Microchemical Journal*.**124**: 646-656

Han, J.H. & Floros, J.D. (1997) Casting antimicrobial packaging films and measuring their physical properties and antimicrobial activity, *Journal of Plastic Film & Sheeting*, **13**(4): 287–298. doi:10.1177/875608799701300405.

Huang, Z., Liu, C., Feng, X., Wu, M., Tang,Y. & Li, B. (2020). Effect of regeneration solvent on the characteristics of regenerated cellulose from lithium bromide trihydrate molten salt. *Cellulose*. **27**: 9243-9256

Loo, C.P.Y. & Sarbon, N.M. (2020) Chicken skin gelatin films with tapioca starch, *Food Bioscience*, **35**, p. 100589. Available at: https://doi.org/10.1016/j.fbio.2020.100589.

Marichelvam, M. K., Jawaid, M. & Asim, M. (2019). Corn and rice starch-based bio-plastics as alternative packaging materials. *Fibers*, **7**(4).doi:10.3390/fib7040032

Md Salim, R., Asik, J. & Sarjadi, M.S. (2021). Chemical functional groups of extractives, cellulose and lignin extracted from native Leucaena leucocephala bark. *Wood Science and Technology*, **55**: 295-313.

Müller, C.M.O., Laurindo, J.B. & Yamashita, F. (2009) Effect of cellulose fibers on the crystallinity and mechanical properties of starch-based films at different relative humidity values, *Carbohydrate Polymers*, **77**(2): 293–299. doi: 10.1016/j.carbpol.2008.12.030.

Niu, X., Ma, Q., Li, S., Wang, W., Ma, Y., Zhao, H., Sun, J. & Wang, J. (2021). Preparation and Characterization of Biodegradable Composited Films Based on Potato Starch/Glycerol/Gelatin. *Journal of Food Quality*. doi:10.1155/2021/6633711

Nordin, N., Othman, S.H., Basha, R. & Rashid, S (2018). Mechanical and thermal properties of starch films reinforced with microcellulose fibers. *Food Research*, **2**(6), 555-563. doi:10.26656/fr.2017.2(6).110.

Oladipo, G.O., Awosanya, A., Alayande, S.O., Olutayo, K. O., Isaiah, A. A., Mosaku, A. M., Ilesanmi, N.Y., & Akinlabi, A.K. (2023). Investigation of microcrystalline cellulose extracted from *Thaumatococcus danielli* and *Ficus exasperata* leaves. *Journal of Chemical Society*

of Nigeria, **48**: 691-703.

Abdul Khalil, H.P.S., Chaturbhuj, K. Asniza, S.M., Ying Y.T., Mohammad, R., Nurul, F, Muhammad I.S., Hashim M.F., Abdul F.I.Y., Mohamad K.M.H., Mohd A.K. & Noorul L.M.S. (2017) Nanofibrillated cellulose reinforcement in thermoset polymer composites. *In: Cellulose-Reinforced Nanofibre Composites*, 1–24. doi:10.1016/b978-0-08-100957-4.00001-2.

Pourjafar, M. (2017) Determination of some physical properties of dried jujube fruit, *IRA-International Journal of Applied Sciences*, **8**(2), p. 48. doi:10.21013/jas.v8.n2.p1.

Raju,V., Revathiswaran, R., Subramanian, S., Parthiban, K.T., Chandrakumar, K., Anoop, E.V. & Chirayil, C.J. (2023). Isolation and characterization of nanocellulose from selected hardwoods, viz., *Eucalyptus tereticornis* Sm. and *Casuarina equisetifolia* L., by steam explosion method. *Scientific Reports*, **13**: 1199

Reddy,K.O. Maheswari ,C.U., Dhlamini, M.S. & V.P. Kommula (2016). Exploration on the characteristics of cellulose microfibers from Palmyra Palm Fruits. *International Journal of Polymer Analysis and Characterization*, **21**(4):286–295.doi:10.1080/1023666X.2016.1147799.

Rosli, N.A., Ahmad, I. & Abdullah, I. (2013)**.** Isolation and Characterization of Cellulose Nanocrystals from Agave angustifolia Fibre. *BioResources*, **8**: 1893-1908

Sariningsih , N., Putra, Y P , Pamungkas, W.P. & Kusumaningsih,T. (2018). Edible film from polyblend of ginger starch, chitosan, and sorbitol as plasticizer. *IOP Conference Series: Materials Science and Engineering,* **333**, 012083. doi:10.1088/1757-899X/333/1/012083.

Savadekar, N.R. & Mhaske, S.T. (2012) Synthesis of nano cellulose fibers and effect on thermoplastics starch based films, *Carbohydrate Polymers*, **89**(1):146–151. doi:10.1016/j.carbpol.2012.02.063.

Sayakulu, N.F. & Soloi, S. (2022). The Effect of Sodium Hydroxide (NaOH) Concentration on Oil Palm Empty Fruit Bunch (OPEFB) Cellulose Yield. *In Journal of Physics: Conference Series*, 2314: 012017

Sobini, N., Arampath, P. C., Anuluxshy, B. & Srivijeindran, S. (2022). Development and characterization of Palmyrah (*Borassus flabellifer* L.) tuber starch incorporated biodegradable packaging film. *Journal of Food and Agriculture,* **15**(2), 47. doi: 10.4038/jfa.v15i2.5273

Terinte, N., Ibbett, R. & Schuster, K.C. (2011)**.** Overview on native cellulose and microcrystalline cellulose I structure studied by X-ray diffraction (WAXD) *Comparison between measurement techniques*. **89**: 118-131.

Tongdeesoontorn, W., Mauer, L. J., Wongruong, S., Sriburi, P. & Rachtanapun, P. (2012). Mechanical and physical properties of cassava starch-gelatin composite films. *International Journal of Polymeric Materials and Polymeric Biomaterials*, **61**(10): 778–792. doi:10.1080/00914037.2011.610049

Yang, Y., Li, J., Chen, B., Dong, Y. & Li, Y. (2022). Symmetric and asymmetric vibrations of rotating GPLRC annular plate, International Journal of Mechanical Sciences, 250, https://doi.org/10.1016/j.ijmecsci.2023.108282

Yudha, V., Rochardjo, Jamasri1, H. S. B. J. Widyorini, R., Yudhanto, F. & Darmanto, S. (2021)**.** Cellulose microfibers from salacca midrib fiber isolated by the mechanical treatment. *Jurnal Selulosa*, 11: 1-8